

Simulation study of two-dimensional phase transitions of argon on graphite surface and in slit micropores

Eugene A. Ustinov · Duong D. Do

Received: 18 May 2013 / Accepted: 11 September 2013 / Published online: 22 September 2013
© Springer Science+Business Media New York 2013

Abstract Molecular simulation has been increasingly used in the analysis and modeling of gas adsorption on open surfaces and in porous materials because greater insight could be gained from such a study. In case of homogeneous surfaces or pore walls the adsorption behavior is often complicated by the order–disorder transition. It is shown in our previous publications (Ustinov and Do, *Langmuir* 28:9543–9553, 2012a; Ustinov and Do, *Adsorption* 19:291–304, 2013) that once an ordered molecular layer has been formed on the surface, the lattice constant depends on the simulation box size, which requires adjusting the box dimensions parallel to the surface for each value of loading. It was shown that this can be accomplished with the Gibbs–Duhem equation, which results in decreasing lattice constant with an increase of the amount adsorbed. The same feature is expected to be valid for gas adsorption in narrow pores, but this has not been analyzed in the literature. This study aims at an extension of our approach to adsorption in slit graphitic pores using kinetic Monte Carlo method (Ustinov and Do, *J Colloid Interface Sci* 366:216–223, 2012b). The emphasis rests on the thermodynamic analysis of the two-dimensional (2D) ordering transition and state of the ordered phase; if the ordered phase exists in narrow slit pores, simulation with constant volume box always leads to erroneous results, for example, seemingly incompressible adsorbed phase. We proposed a new approach that allows for modeling

thermodynamically consistent adsorption isotherms, which can be used as a basis for further refinement of the pore size distribution analysis of nanoporous materials.

Keywords Kinetic Monte Carlo · Adsorption on graphite · Monolayer phase transition · Heat of adsorption · Slit pores

1 Introduction

Two-dimensional (2D) ordering transition in the adsorbed phase is a challenging task which still experiences difficulties in its quantitative description with molecular simulation methods. There are a large number of publications devoted to the analysis of the formation of the 2D crystal-like phases on homogeneous surfaces (mainly graphite), at sufficiently low temperatures (Migone et al. 1984; Larese et al. 1989; D’Amico et al. 1990; Flenner and Etters 2002, 2006). Below the 2D triple point there is a co-existence of the gas and solid phases at sub-monolayer coverages. For temperatures in the range between the 2D triple point and the 2D critical temperature there could be the 2D gas–liquid and 2D liquid–solid transitions, depending on the tangential pressure. Above the 2D critical temperature only the 2D hypercritical fluid–solid can exist (Morrison 1987). In this study we focus on the 2D liquid–solid and 2D hypercritical fluid–solid transitions, which can be viewed as an ordering transition. A convincing calorimetric evidence of such a transition has been shown with Ar/N₂–graphite systems at 77 K (Rouquerol et al. 1977; Grillet et al. 1979). In the case of argon this temperature exceeds the 2D triple point by nearly 30°. There is a prominent spike in the heat curve versus loading, corresponding to the ordering transition just after the completion of the

E. A. Ustinov (✉)
Ioffe Physical Technical Institute, 26 Polytechnicheskaya,
St. Petersburg 194021, Russia
e-mail: eustinov@mail.wplus.net

D. D. Do
School of Chemical Engineering, University of Queensland,
St. Lucia, QLD 4021, Australia

monolayer, and recently this spike was unambiguously reproduced with Monte Carlo simulation (Fan et al. 2012; Ustinov and Do 2012a, 2013). The heat spike is observed in simulated heat curves up to 89 K (Ustinov and Do 2013). The ordering transition is also seen in experimental adsorption isotherms as a small, but well reproducible kink. Thus, Demetrio de Souza and Lerner (1987) presented sixteen argon isotherms on graphite at temperatures from 54 to 89 K. The kink corresponding to the 2D ordering transition is visible for temperatures in the range from 63 to 84 K. At 77 K the two-dimensional ordering transition is observed for nitrogen and argon adsorption on graphitized carbon black at around 0.8 and 1.2 kPa, respectively (see, for example, Kruk et al. 1999; Gardner et al. 2001). The ordering transition presents a challenge for its correct description with a molecular simulation because of the strong correlation between the lattice constant and the simulation box dimensions when the periodic boundary conditions are applied. If the box volume is kept constant and it is not too large, the lattice constant of the ordered monolayer is also constant regardless of the bulk pressure resulting in its constant density, which contradicts the increase of monolayer density as pressure is increased. This effect is especially important for modeling of adsorption of gases in narrow pores where the adsorbed phase can be completely ordered. In this case using a conventional molecular simulation technique with a constant volume box would lead to a horizontal section of the adsorption isotherm at high pressures, as if the adsorbed phase is incompressible. Depending on the box size and other factors, the ordered molecular layers on an open surface or in a slit pore can rotate to decrease the lattice constant in order to accommodate further molecules. As a result, the density of the adsorbed phase would exhibit a small step increase, at a pressure that is not reproducible. Furthermore, if the symmetry axes of the lattice are not parallel to the side of the simulation box, periodic boundary conditions will not provide a defect free extension of the lattice outside the box. All drawbacks of Monte Carlo simulation in the box of constant size can be seen in a recent paper of Abaza et al. (2012). Adsorption isotherms simulated by the authors show artificial substeps and oscillations due to spontaneous rearrangement of the defected crystalline monolayer with the insertion of molecules to the adsorbed phase. Significant oscillations are also seen in the isosteric heat, which sometimes makes excursion into the negative region.

To overcome this deficiency we proposed a method based on the matching of the tangential pressures determined with the ‘mechanical’ and ‘thermodynamic’ routes (Ustinov and Do 2012a). The former was done with the virial equation of Irving and Kirkwood (1950). Thermodynamically the tangential pressure was determined as the

difference between the Gibbs and Helmholtz free energies per unit volume, with the latter obtained by integration of the chemical potential with respect to the number of molecules along the adsorption isotherm. These two pressures are exactly the same before the ordering transition occurs and, after the transition, they deviate from each other by up to 100 % if the box volume is fixed. For each loading, there are specific box sizes for which the pressures calculated from two different routes are the same. Those sizes were proved to correspond to the Helmholtz free energy minimum, resulting in a thermodynamically correct relationship between the amount adsorbed and the lattice constant. A series of argon adsorption isotherms simulated in the box of various fixed sizes at 77 K revealed a dependence of the lattice constant on loading, which was then used in the simulation for the thermodynamically consistent adsorption isotherm in the box of variable size. A less time-consuming approach was further developed on the basis of Gibbs–Duhem equation (Ustinov and Do 2013). In this approach the simulation box volume is corrected for each loading so that the difference between the chemical potential and the tangential pressure obey the Gibbs–Duhem equation. In both procedures the monolayer density increases with the increase of chemical potential as one would expect physically. Technically, instead of the box size correction one can use a finite pore in the *xy*-plane. In this case the adsorbed phase is in direct contact with the bulk phase, which allows for self-adjusting of the lattice constant at given parameters. This technique was realized by Long et al. (2013), but they did not study the lattice defects, dislocations and rotation of the 2D crystal-like relative to the box, which could be a source of some uncertainties.

In the present study we rely on the Gibbs–Duhem equation to determine thermodynamic parameters of the order–disorder transition in slit pores and to predict the chemical potential in the region where the adsorbed phase is completely ordered. This is distinct from our previous studies (Ustinov and Do 2012a, 2013) for argon adsorption on graphite. In those studies the parameters of the disorder-to-order transition were determined approximately within the van-der-Waals loop of the canonical adsorption isotherm using a smoothing procedure based on the grand canonical partition function. However, that method is inapplicable in the case of adsorption in narrow pores. This is because of uncertainty of the chemical potential for the completely ordered phase (see explanations in Sect. 3.2). For the same reason the well-known Maxwell rule of equal areas cannot be applied to describe the order–disorder transition. To overcome this difficulty we derived an equivalent rule of equal areas by integration of the Gibbs–Duhem equation, which involves the reliably determined tangential pressure instead of the chemical potential. Further integration of the Gibbs–Duhem equation over the

region of higher densities allowed for the determination of the chemical potential of the crystal-like adsorbed phase. In some cases we also provided a comparison of results obtained with the canonical and the grand canonical kinetic Monte Carlo (kMC), which was recently developed (Ustinov and Do 2012c).

2 Methodology and simulation details

We present a methodology of analysis of gas adsorption on open homogeneous surfaces and in slit pores, and used Ar—graphite and Ar—slit graphitic pores as examples to illustrate this methodology. In the case of the Ar—graphite system we generally adhere the methodology described previously (Ustinov and Do 2012b, 2013) and based on simulation with the kMC scheme and the Gibbs–Duhem equation for the lattice constant determination. However, in this paper we implemented the approach by simulation in a grand canonical ensemble (GCE) in the framework of the kMC (Ustinov and Do 2012c). With this new approach, we avoided the significant jump in chemical potential in the region just after the completion of the first layer when the adsorption isotherm is simulated in a canonical ensemble at low temperatures. It was shown that the addition only a few molecules to the system lead to a strong contraction of the monolayer and the chemical potential jumps toward a much higher value, which hampers the application of the Gibbs–Duhem equation. This is the reason why application of the grand canonical version of kMC (GC-kMC) provides more reliable results for the chemical potential is an independent variable which can be incremented by a small step.

The second task is a determination of thermodynamic functions of the ordered and disordered phases in coexistence, in particular, the lattice constant at the instant of the appearance of the ordered phase. This value of the lattice constant is a starting point for the Gibbs–Duhem integration and an incorrect choice of this value would lead to a thermodynamic inconsistency of the ordered phase at any bulk pressure. In case of a 2D gas–liquid phase transition its parameters can be easily found by using the condition of equality of the tangential pressure and the chemical potential for these coexisting phases. However, this is not enough in case of the 2D liquid–solid phase transition because those equalities can be provided at various values of the lattice constant defined by L_x and L_y dimensions of the simulation box. In order to overcome this uncertainty we additionally used the Maxwell rule of equal areas in the region of phase transition. This technique is quite cumbersome, but it allowed us to determine the lattice constant of the ordered layer coexisting with the 2D liquid-like layer as a function of temperature.

We paid a special attention to argon adsorption in narrow commensurate slit pores. In this case, once the ordering transition has occurred, an increase in the specific amount adsorbed is only possible with a decrease of the lattice constant. This can be accomplished at a constant number of molecules in the simulation box by decreasing the dimension L_x and keeping the ratio $L_y/L_x = 3^{1/2}/2$. A common way to increase the number of molecules at a constant box volume would inevitably result in the appearance of lattice defects and dislocations. We develop a new technique to describe the ordering transition in the slit pore based on the Gibbs–Duhem equation:

$$Nd\mu = Vd\bar{p}_T \quad (1)$$

Here N is the number of molecules in the system of volume V , μ is the chemical potential, and \bar{p}_T is the tangential pressure averaged along z -direction over the range $0 < z < L_z$. The reason why only the tangential pressure is used in (1) is that at a constant pore width and number of molecules in the box the work is produced only by this component of the pressure tensor when the box volume is changed. Eq. (1) can be rewritten as

$$\rho d\mu = d\bar{p}_T \quad (2)$$

where $\rho = N/V$ is the average density of the adsorbed gas in the pore. In the region of phase transition the pressure does not depend on composition of the binary system. Therefore, in the limit of the 2D phase transition where one of the two phases disappears, the corresponding pressures must be the same regardless of whether the system is open or closed. Then the integration of Eq. (2) along the van der Waals-type loop obtained in a canonical ensemble immediately leads to the Maxwell rule of equal areas. Similarly, using equality of the chemical potential at the starting and ending points of the ordering transition, one can obtain the following equation:

$$\oint_{ODE} \rho^{-1} d\bar{p}_T = 0 \quad (3)$$

Here ODE denotes the order–disorder equilibrium. Equation (3) can be rearranged as follows:

$$\varphi_D = \varphi_O \quad (4)$$

where

$$\varphi = \xi + \int_{\rho_0}^{\rho} \frac{\xi}{\rho} d\rho \quad (5)$$

Here subscripts ‘D’ and ‘O’ denote states of the liquid or hypercritical fluid (disordered) and the solid (ordered) 2D phases at the starting and ending points of the transition, respectively, $\xi = \bar{p}_T/(\rho k_B T)$ is the dimensionless

compressibility factor, k_B is the Boltzmann constant, T is the temperature, and ρ_0 is a reference value. The plot $\varphi - \rho\xi$ has a point of intersection, which corresponds to the order–disorder coexistence when $\varphi_D = \varphi_O$ and simultaneously $(\rho\xi)_D = (\rho\xi)_O$. Note that $\rho\xi$ is proportional to the tangential pressure at a given temperature.

Using Eq. (3) instead of the Maxwell rule is more reliable in the case when a complete crystal-like adsorbed phase appears as a result of the 2D phase transition without a disordered phase. Thus, if the simulation is performed in a canonical ensemble, a conventional way of determination of the chemical potential (for example, the Widom method) is highly sensitive to the change of number of molecules relative to the number of lattice sites. Therefore, to maintain the physical nature of chemical potential as the partial derivative of Helmholtz free energy with respect to number of molecules it is necessary to use an extremely large simulation box, otherwise the chemical potential would be uncertain. On the other hand, the tangential pressure determined with the virial route is nearly insensitive to a small difference between the number of molecules and the number of lattice sites in the box, which makes Eq. (3) more preferable to the Maxwell rule for evaluation of the order–disorder parameters. In doing so, the chemical potential can be determined by integration of the Gibbs–Duhem Eq. (2), which means that the chemical potential is proportional to φ defined by (5).

Based on this analysis, we developed a following procedure to calculate the gas adsorption isotherm in narrow slit pores. Initially at a given temperature T we formed a hexagonally packed adsorbed phase consisted of one or two molecular layers depending on the slit pore width, with the number of molecules being equal to the number of lattice sites. The box size was chosen so that the ordered adsorbed phase was stable. Then we performed a series of consecutive canonical kMC simulation runs with box size in the L_x dimension incremented by ΔL_x while keeping the ratio L_y/L_x of $3^{1/2}/2$. When the dimension L_x exceeded some critical value, the ordered structure of the adsorbed phase is instantly destroyed and the further increase of the box volume provided modeling of the adsorption isotherm for the disordered adsorbed phase. The number of lattice sites for the monolayer was taken equal to 400 both in case of adsorption on the open surface and in pores. The number of kMC steps was 25×10^6 for equilibration and 50×10^6 for sampling. All parameters for Ar–Ar and Ar–graphite interactions were taken the same as in our previous works (Ustinov and Do 2012a, 2012b, 2012c, 2013). The periodic modulation of the gas–solid potential due to surface corrugation was neglected due to its insignificant effects on thermodynamic properties of argon on graphite surface and confined in slit pores (see, for example, Long et al. 2013). The second reason of such simplification was motivated by

our objective to analyze the net effect of the 2D disorder-to-order transition in the confined space without any interference of any secondary effects.

3 Results and discussion

3.1 Argon adsorption on graphite surface

As is described in Sect. 2, we determined the lattice constant of the ordered molecular layer coexisting with the 2D liquid or 2D hypercritical fluid using the Maxwell rule of equal areas and the condition of equality of the tangential pressure and the chemical potential of the coexisting phases. Figure 1 shows the lattice constant and the tangential pressure as a function of temperature.

As seen in Fig. 1, the lattice constant decreases with temperature. This means that the monolayer density increases with temperature, which at first seems surprising, however it is noted that the coexisting tangential pressure also increases with temperature, which induces the densification of the monolayer. Generally, the ordering transition is a response of the system with the increase of tangential pressure. From this viewpoint it is clear that at a higher temperature the ordering transition can be induced by a higher tangential pressure. In Fig. 1 the tangential pressure is multiplied by the dimension L_z . This value has the same dimension as the surface tension and its advantage is that it is essentially independent of L_z for sufficiently large L_z .

At a given temperature the lattice constant of the 2D ordered phase coexisting with the disordered 2D gas or liquid phase is the starting point for further integration of the Gibbs–Duhem equation along the adsorption isotherm. Thus, at 77 K the lattice constant is $1.1537\sigma_{ff}$, so if we choose 400 sites of the hexagonal lattice inside the

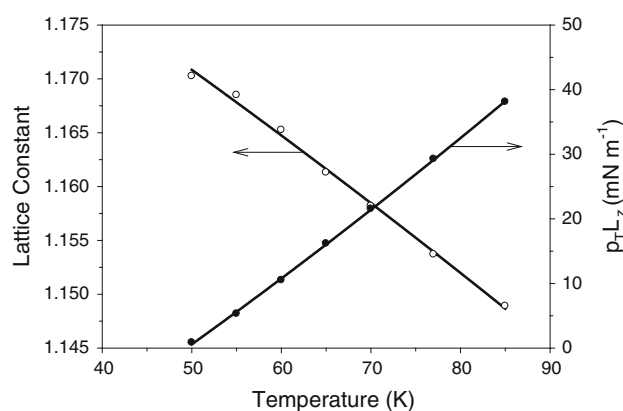


Fig. 1 Variation of the lattice constant (white circle) and the tangential pressure (black circle) of the 2D ordered molecular layer with temperature in the system argon–graphite at the order–disorder phase transition. The lattice constant is determined in units of σ_{ff}

simulation box, the initial dimension L_x would be $23.074\sigma_{ff}$. The chemical potential μ_{OD} corresponding to the 2D order–disorder coexistence is presented in Fig. 2 as a function of temperature.

At a given temperature the adsorption system is disordered below the chemical potential μ_{OD} and therefore its behavior can be described by simulation with either canonical (CE) or GCE in a box of constant volume. For chemical potentials greater than μ_{OD} the contact layer is ordered and the adsorbed phase has to be simulated in a box of variable size according to the Gibbs–Duhem equation.

Figure 3 shows argon adsorption isotherms on graphite at 50 and 77 K simulated in canonical and GCEs. In the former case the simulation box was of constant volume having dimension L_x of $23\sigma_{ff}$. In the latter case simulation was accomplished only above the ordering transition in the box of variable size determined with the Gibbs–Duhem equation.

At 50 K the chemical potential determined with a canonical ensemble increases significantly (by 8.9 kT) just after the formation of the continuous ordered monolayer. Such an artificial gap at constant loading can be avoided with the GCE on a variable simulation box, in which once the graphite surface is fully covered with a layer of molecules the adsorbed density increases sharply with chemical potential (red line in Fig. 3). This is an important result that the solid-like monolayer is compressible, while the simulation in the box of constant volume leads to an apparent incompressibility, which is obviously an artifact resulted from the constant volume of finite size. The vertical section in the isotherm for 50 K simulated in the GCE correspond to the disorder–order transition between 2D liquid and 2D solid, while that for 77 K is the transition between 2D hypercritical fluid and 2D solid. There is a vertical step in the CE-adsorption isotherm at 50 K in the range from 4 to

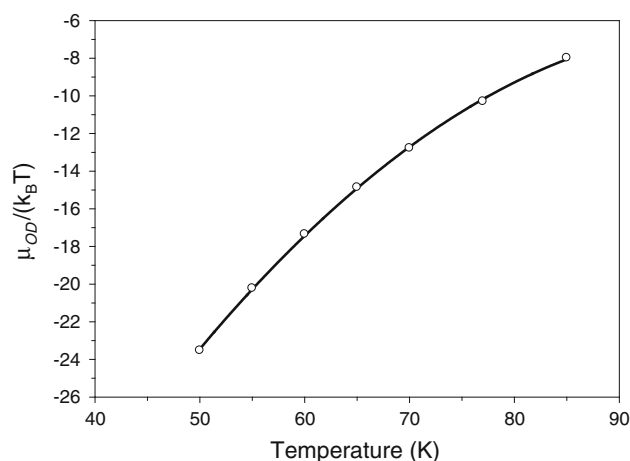


Fig. 2 The chemical potential of the 2D binary order–disorder system versus temperature at argon adsorption on graphite. Hereafter we omit the standard chemical potential $\mu^\circ(T)$ for simplicity

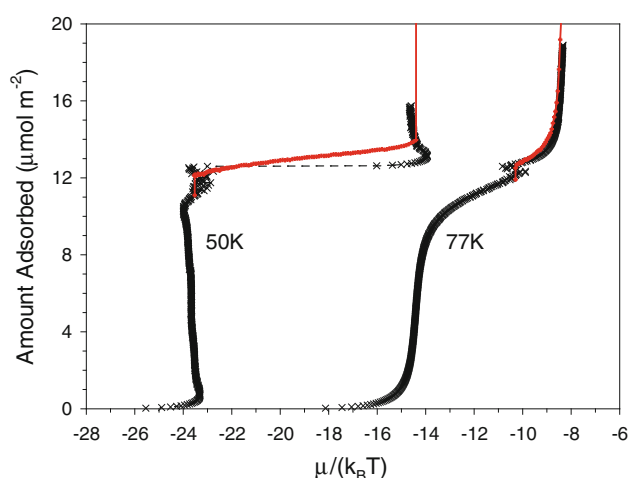


Fig. 3 Argon adsorption isotherms on graphite simulated with the kMC at 50 and 77 K. Black symbols correspond to simulation in a canonical ensemble in a box having constant size ($L_x = 23\sigma_{ff}$). Red symbols are the result of simulation in a GCE in a variable box

$7.5 \mu\text{mol}/\text{m}^2$, which corresponds to the 2D vapor–liquid transition because 50 K is between the 2D triple point and the 2D critical temperature of 63 K (Ustinov and Do 2013). The 2D vapor–liquid and liquid–solid transitions occur at the chemical potential of $-23.67k_B T$ and $-23.53k_B T$, respectively. Such a small difference is due to the proximity of 50 K to the 2D triple point (which was found to be 47.2 K for the case where the modulation of the graphite potential is neglected (Ustinov and Do 2013)). Below the triple point there is one transition in the first layer, which is the 2D vapor–solid transition, in distinct from the ordering transition considered in the present study.

The effect of the box size variation is also seen in the 77 K adsorption isotherm. Once the ordering transition has occurred, the thermodynamically correct isotherm is higher than that simulated in the box of constant volume.

Figure 4 presents the dependence of the box dimension L_x on the chemical potential in the region where the monolayer is ordered.

The variation of the simulation box size occurs mainly after the ordering transition. Our tentative results seem to suggest that regardless of the temperature the lower limit of the lattice constant is $\sim 1.11\sigma_{ff}$, which is close to that corresponding to the mechanical equilibrium of the infinite 2D Lennard–Jones lattice at zero temperature equaled to $1.115\sigma_{ff}$ (Ustinov and Do 2012a).

The comparison of simulated argon adsorption isotherm on graphitized carbon black at 77 K with experimental data of Gardner et al. (2001) is shown in Fig. 5.

Experimental and simulated data for the system Ar–graphite at 77 K presented in Fig. 5 are in good agreement, with no adjusting parameters being used. Some deviations are observed and this is due to the fact that multibody

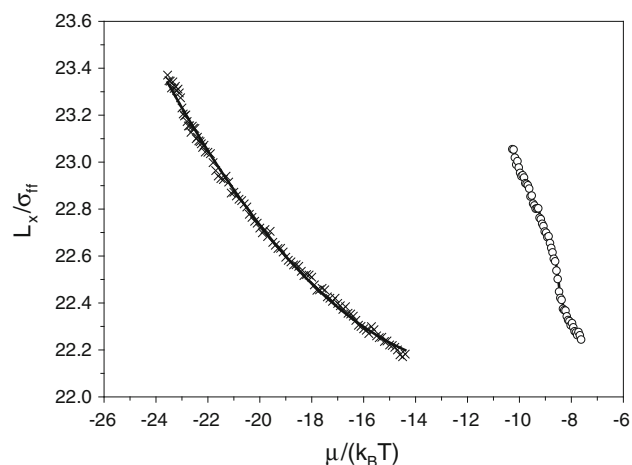


Fig. 4 The dimension L_x of the simulation box as a function of the chemical potential, which ensures thermodynamic correctness of the system Ar–graphite in case of formation of the ordered monolayer at 50 K (times) and 77 K (white circle)

interactions are not accounted for, which slightly smooth and shift the phase transition steps toward higher bulk pressures (Ustinov et al. 2011). The most important feature is that the kink on the experimental adsorption isotherm indicating the 2D ordering transition (Fig. 5b) is reproduced by simulation reasonably well, validating our methodology.

3.2 Argon adsorption and ordering transition in slit pores

According to the procedure described in Sect. 2, we carried out two simulations for each temperature. The first

simulation was performed in a canonical ensemble with a rectangular box of constant volume to model disordered adsorbed phase. In the second one the amount adsorbed was varied by allowing the box volume to vary at a constant number of molecules. Initially a hexagonal structure of the adsorbed phase was created, with the number of molecules being equal to the number of lattice sites. The ratio L_y/L_x was kept constant at $3^{1/2}/2$. Simulations were carried out mainly with 400 molecules in one molecular layer. In the present paper we focused on slit pores whose widths are two and three times the collision diameter of argon. Such pores can accommodate one and two molecular layers, respectively, so in the latter case the number of molecules in the simulation box was 800. The conventional periodic boundary conditions were used.

Figure 6a shows a section of argon adsorption isotherm in slit pore of $2\sigma_{ff}$ width at 77 K in the form of the amount adsorbed versus the tangential pressure.

As seen in Fig 6a, there are two branches of the isotherm corresponding to the ordered and disordered adsorbed phases. The equilibrium transition between these two phases is determined from the intersection between the plots of the group $\varphi/(\bar{p}_T L_z)$ versus $\bar{p}_T L_z$ (see Eqs. 4 and 5) as shown in Fig. 6b for the ordered and disordered adsorbed phases. At the point of intersection two conditions for the phase coexistence are satisfied simultaneously, namely, $\varphi_O = \varphi_D$ and $\bar{p}_{TO} = \bar{p}_{TD}$, where the subscripts O and D denote the ordered and disordered phases, respectively. The same result can also be obtained from the $\varphi - \bar{p}_T L_z$ plots, but it is less convenient in terms of visualization because of much wider range of the function φ compared to $\varphi/(\bar{p}_T L_z)$.

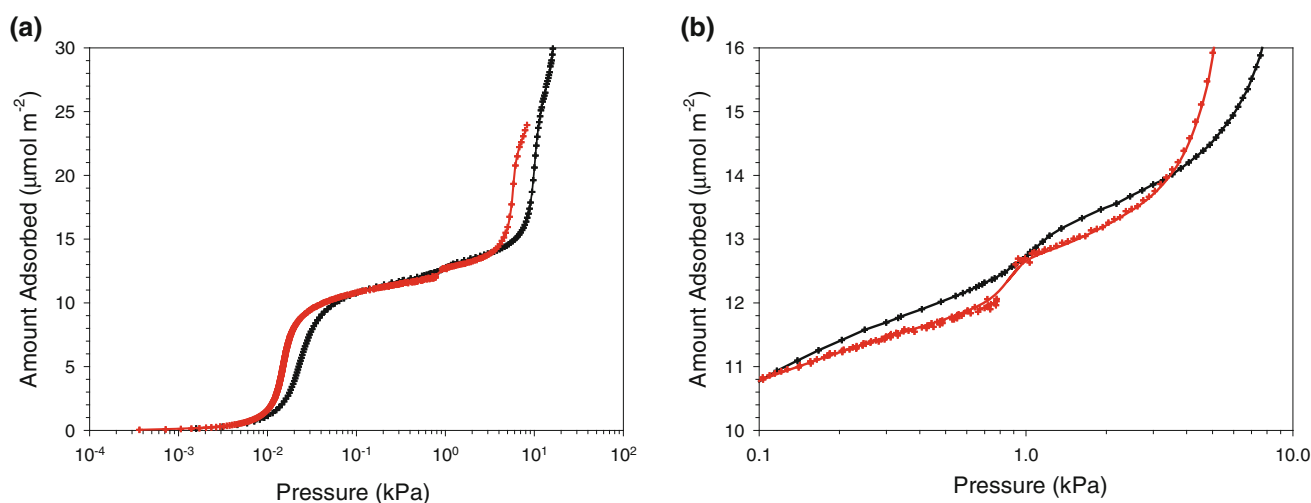


Fig. 5 Argon adsorption isotherm on graphitized carbon black at 77 K in the normal (a) and enlarged scale (b) in the area of the 2D phase transition. Black points are for the experimental data of Gardner et al. (2001). Red points are simulated data. The red line is the result

of smoothing the simulated isotherm with the grand canonical distribution applied for the box, which allows for 400 lattice sites in the ordered argon monolayer

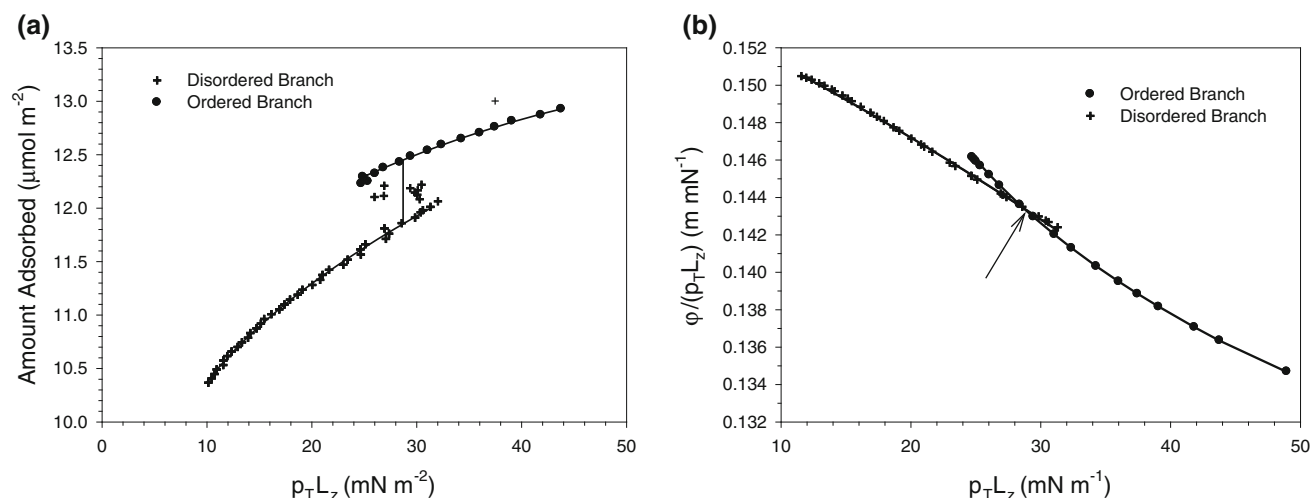


Fig. 6 **a** The amount adsorbed versus tangential pressure in the system Ar—slit pore of $2\sigma_{ff}$ (0.679 nm) at 77 K. The simulation is performed in a variable box with 400 molecules. **b** A scheme used for determination parameters of the 2D ordering transition. The branches

The scheme proposed for the determination of the 2D order–disorder equilibrium transition resembles that based on the analysis of the Ω – μ curve, where Ω is the grand thermodynamic potential. However, the latter is not appropriate in our problem because both Ω and μ cannot be reliably determined with molecular simulation when the adsorbed phase is completely ordered as shown in Fig. 7 where we plotted the chemical potential versus the function ϕ .

An important result arising from Fig. 7 is that the function ϕ is thermodynamically identical to the chemical potential for the disordered branch of the adsorption isotherm because the plot $\mu/(k_B T) - \phi$ is a straight line with the slope of unity.

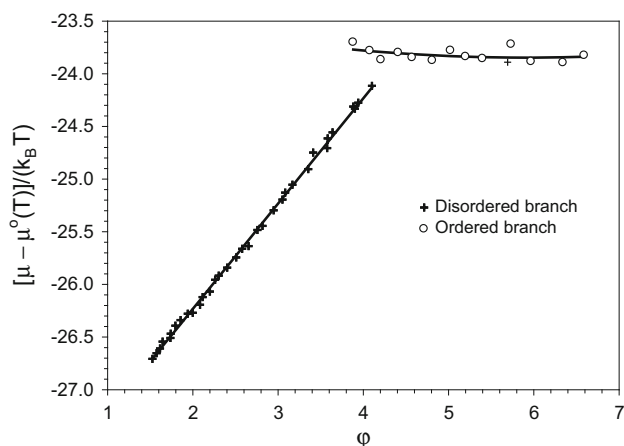


Fig. 7 The chemical potential versus the function ϕ in the system Ar—slit pore of $2\sigma_{ff}$ (0.679 nm) at 77 K. For the disordered branch (plus) the plot is a straight line with the slope of exactly $\pi/4$, which means that $k_B T \phi$ is an alternative expression of the chemical potential. In the region of the ordered adsorbed phase the chemical potential (white circle) determined with the kMC is nearly constant which is incorrect

for the ordered and disordered phases in coordinates of this figure have a single point of intersection (shown by arrow), which corresponds to the 2D order–disorder coexistence

Interestingly, the expression in Eq. (5) for ϕ involves only the tangential pressure despite the normal pressure in 0.679 nm slit pore is not negligible as in the case of adsorption on the graphite surface and its value of 47.5 MPa is comparable to the tangential pressure. What seems surprising is that the chemical potential for the ordered adsorbed phase determined with the kMC simulation changes insignificantly with the amount adsorbed. Similar results were also obtained with the Widom test particle insertion method. The reason why any molecular simulation technique fails to determine the chemical potential of a highly ordered phase correctly is because of a relatively small simulation box. As was mentioned in Introduction, the chemical potential is a partial variable, which implies that insertion or rejection of one molecule results in a small change in the Helmholtz free energy and other thermodynamic potentials. However, it is not the case if the adsorbed phase is completely ordered because its properties are strongly dependent on a small difference between the number of lattice sites and the number of molecules. For example, if all lattice sites are filled the behavior of an extra molecule would be drastically different compared to all other molecules because of strong repulsion between that molecule and the existing molecules on the lattice sites. On the other hand, the tangential pressure is weakly dependent of a small change in the number of molecules and is determined reliably with a straightforward virial route. It allows us to suggest that the function ϕ maintains its physical meaning in the region of an ordered phase and the value $k_B T \phi$ should be used instead of the chemical potential.

Figure 8a presents a composite argon adsorption isotherm for the 0.679 nm slit pore. It is composed of the

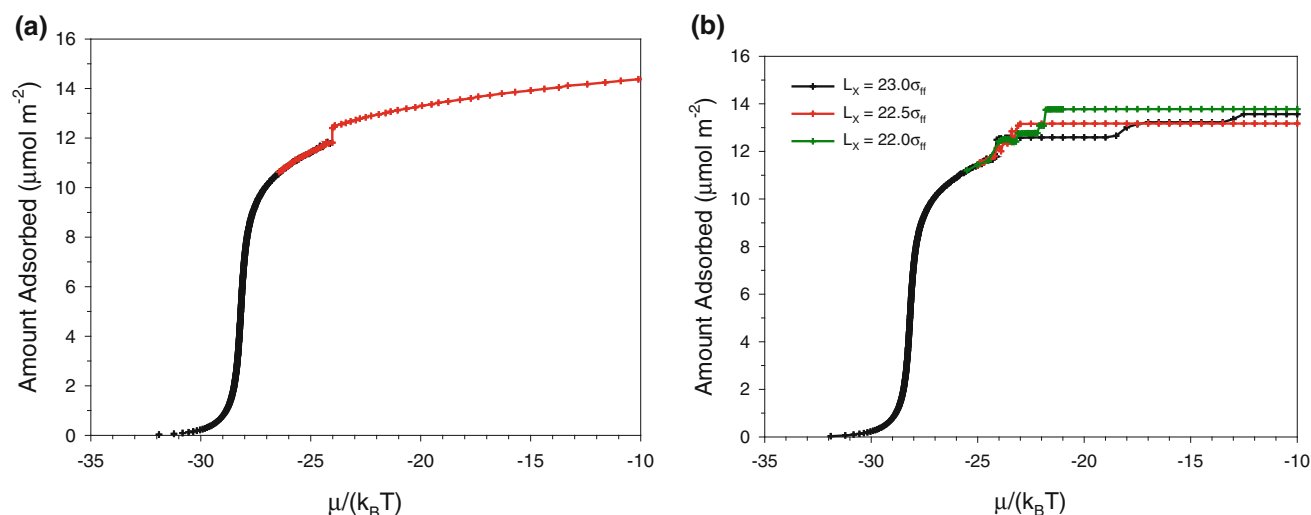


Fig. 8 Argon adsorption isotherm in slit pore of $2\sigma_{ff}$ (0.679 nm) at 77 K. **a** The section plotted by black line is simulated in a canonical ensemble in a box of constant volume. The red line is the adsorption isotherm simulated in a box of variable size with 400 molecules.

b The upper parts of the adsorption isotherm are simulated in the GCE in the simulation box of constant volume. The L_x dimension for each isotherm is shown in the legend

isotherm simulated in a canonical ensemble with constant volume up to the ordering transition and the isotherm simulated in the variable box.

As seen in Fig. 8a, in the region of disordered adsorbed phase the isotherm does not depend on the box size and is insensitive of whether the box volume is constant or not. To the right of the vertical step corresponding to the disorder–order transition the isotherm was plotted using Eq. (5) for the chemical potential. One of the significant results from this simulation is that the ordered adsorbed phase is compressible. It is instructive to compare this composite isotherm with that obtained with a GCE of constant volume, which is shown in Fig. 8b. We see that the GCE-isotherm is a strong function of the box size in the region of ordered adsorbed phase, which is clearly an artifact, resulted from the finite box size. As a corollary of this artifact is the plateau of the GCE-isotherm after the transition, creating an erroneous impression that the crystalline adsorbed phase is incompressible. Moreover, the phase transition step splits into several sub-steps, which is due to instant rotation of the monolayer lattice relative to the box. Sometimes such rotation could occur at a much higher chemical potential (see the black line in Fig. 8b) resulting in kinks which resemble phase transitions.

Argon adsorption isotherm simulated at 77 K in $3\sigma_{ff}$ (1.018 nm) slit pore is shown in Fig. 9.

The adsorbed phase consists of two molecular layers and, again, the ordered phase is compressible. The vertical step of the adsorption isotherm within zone A is resulted from the vapor–liquid coexistence, which was not observed at the same temperature in the narrower pore accommodated only one molecular layer. This is because the 2D

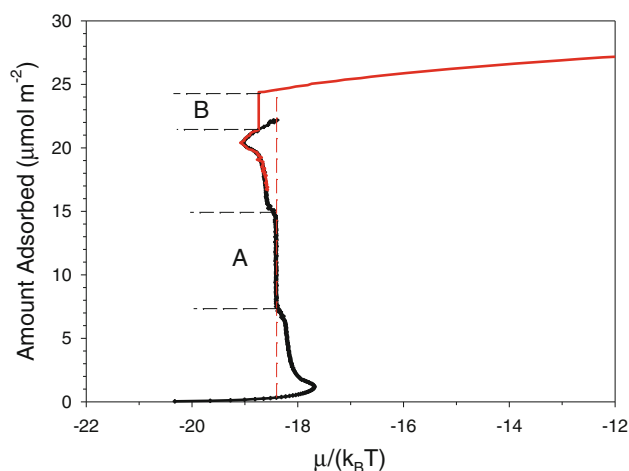


Fig. 9 Argon adsorption isotherm in slit pore of $3\sigma_{ff}$ (1.018 nm) at 77 K. The black line represents the isotherm simulated in a canonical ensemble in a box of constant volume. The red line is the adsorption isotherm simulated in a box of variable size with 800 molecules. Zone A is the 2D vapor–liquid coexistence. Zone B is the liquid–solid coexistence

critical temperature is greater with larger pore. Zone B corresponds to the 2D liquid–solid transition. Interestingly, the liquid–solid transition occurs at a lower chemical potential than the vapor–liquid transition does. Therefore, if argon is introduced to the system by small doses, one could first observe the vapor–liquid transition, with the vapor-like region shrinks as loading is increased until the liquid-like region completely fills the pore. Further doses will result in solidification of the liquid phase. However, in an open system only vapor–solid transition can occur along the dashed vertical line shown in Fig. 9.

We showed in Fig. 10 the contour lines of the density distribution averaged over 50×10^6 kMC steps, and observed a commensurate hexagonal packing of the bilayer in this 1.018 nm pore. For better visualization we have used different colors for the first and second layers.

Density distributions presented in Fig. 10a, b correspond to the lower and the upper point of the liquid–solid transition step designated by zone B in Fig. 9.

It should be noted that the ordering transition in slit pores not always leads to the hexagonal packing. If the pore width is not equal to integral number of the molecular

diameter, the square lattice structure appears at sufficiently large loadings (Vishnyakov and Neimark 2003; Salamacha et al. 2004; Kaneko et al. 2010). As an example, Fig. 11 presents argon adsorption isotherm at 77 K in slit pore of $2.6\sigma_{ff}$ (a) and the density distribution of the ordered adsorbed phase (b).

As seen in Fig. 11, the ordering transition also occurs in the pore which does not accommodate an integral number of molecular layers. The distance between the two layers in the pore of $2.6\sigma_{ff}$ at the amount adsorbed of $19.667 \mu\text{mol}/\text{m}^2$ is only $0.67\sigma_{ff}$ which resulted in the formation of the

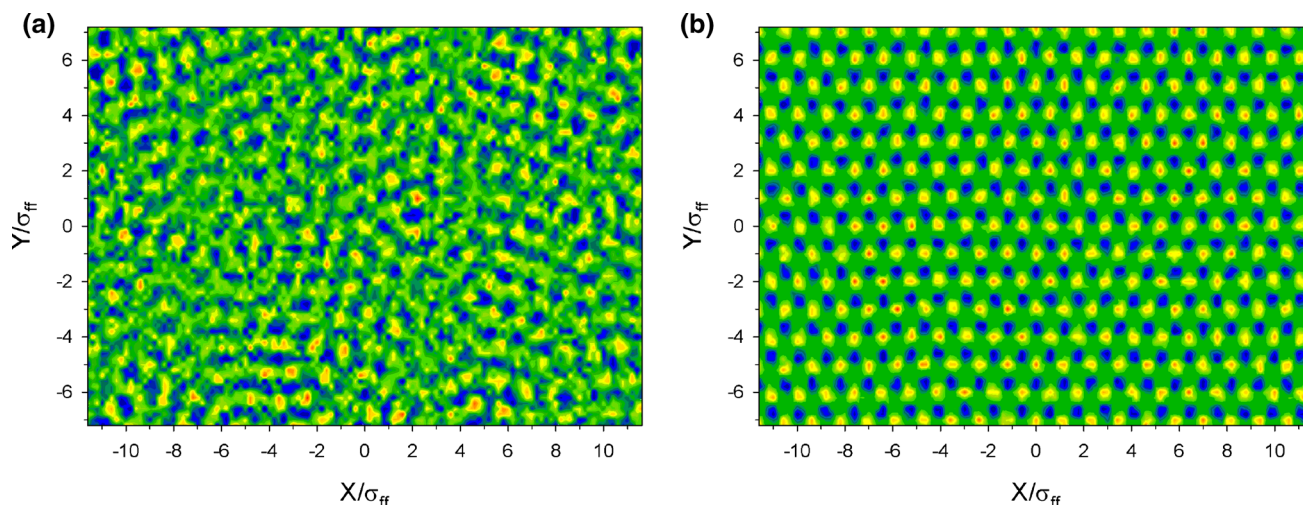


Fig. 10 The contour plot for density distribution of the disordered (a) and ordered (b) argon layer adsorbed in slit pore of 1.018 nm at 77 K. $L_x = 23.35\sigma_{ff}$. The number of molecules is 700 and 800 for the disordered and ordered layer, respectively. Blue and red spots

correspond to molecules of the first and the second molecular layer, respectively. The green color is for zero density. Other explanations are in the text

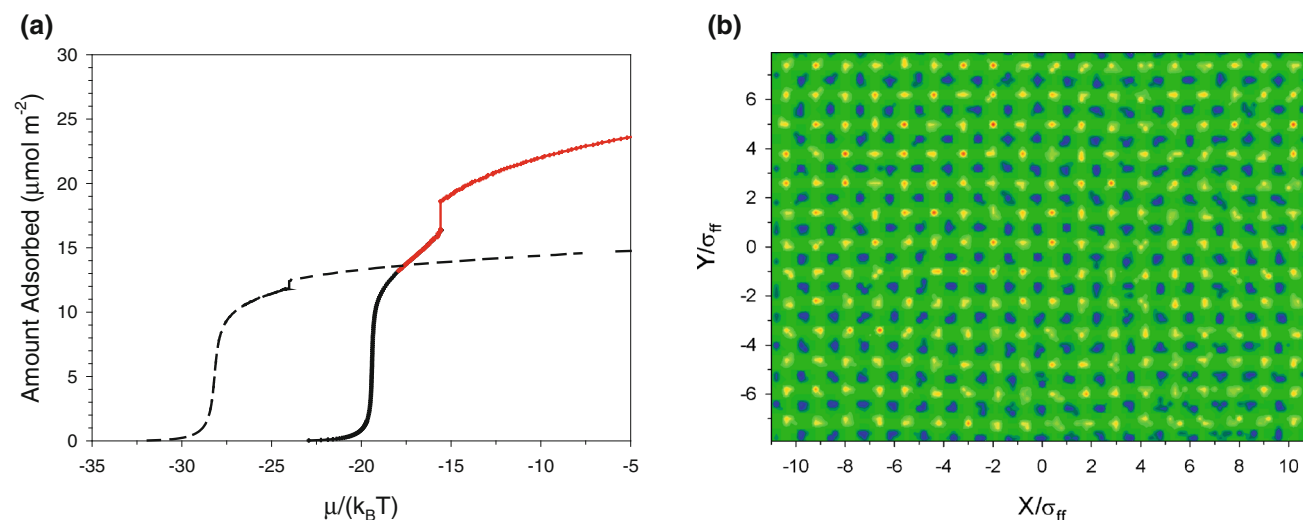


Fig. 11 a Argon adsorption isotherm in slit pore of $2.6\sigma_{ff}$ (0.882 nm) at 77 K. The black line represents the isotherm simulated in a canonical ensemble in a box of constant volume. The red line is the adsorption isotherm simulated in a box of variable size with 800

molecules. The dashed line is the isotherm in $2.0\sigma_{ff}$ pore. b The density distribution of the ordered argon bilayer. $L_x = 21.8\sigma_{ff}$, $N = 800$. Blue and red color correspond to the first and the second layer, respectively. The green line denotes zero density

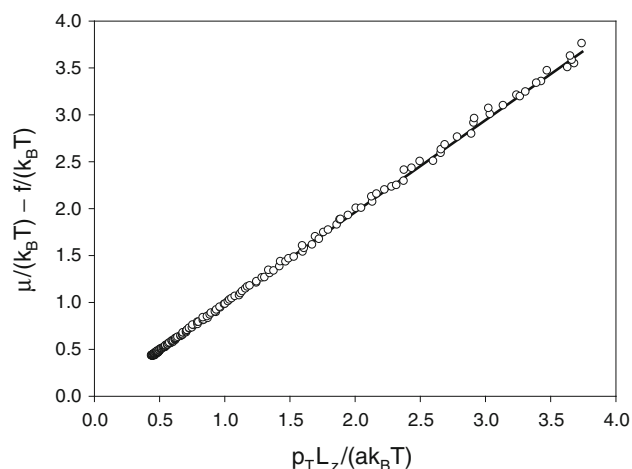


Fig. 12 Correlation of the difference between molecular Gibbs and Helmholtz free energies with the tangential pressure for the system Ar—slit pore of 1.018 nm at 77 K. In this coordinates the correlation is the straight line with the slope of 0.981

square lattice. It should also be mentioned that a relatively small distance between the layers leads to a sharper increase of the normal pressure with loading compared to the case of integral number of layers in the pore.

3.3 Thermodynamics of ordering transition in slit pores

In this Section we consider the behavior of the adsorbed phase and the 2D phase transition from thermodynamic viewpoint in the 0.679 nm slit pore. This pore can accommodate only one molecular layer, but it does present a special case, for which its thermodynamic analysis can be generalized for larger pores at various temperatures.

At the first step we will derive a correlation between the Helmholtz free energy, the chemical potential and the tangential pressure of the adsorbed phase in a slit pore. This issue has been addressed when we dealt with argon adsorption on a graphite surface (Ustinov and Do 2012a). It was shown that the difference between the Gibbs and the Helmholtz free energies is the average tangential pressure times the volume of the system. However, in that case the normal pressure was negligibly small compared to the tangential pressure, which we suspected that this is the reason why the former does not contribute to that difference. In the case of argon adsorption in slit pores the normal component of the pressure tensor is generally comparable with the tangential pressure. Therefore, it is necessary to check whether the normal component can be ignored in thermodynamic functions. To this end, we determined the Helmholtz free energy at any loading within the region of disordered phase by integration of the chemical potential with respect to the amount adsorbed. Then the Helmholtz free energy per molecule is given by

$$f(T) = \frac{1}{a} \int_0^a \mu(T, a_1) da_1 \quad (6)$$

where a is the amount adsorbed. Figure 11 presents the plot $(\mu - f)/(k_B T)$ versus the tangential compressibility factor $\xi = \bar{p}_T L_z / (a k_B T)$.

The correlation shown in Fig. 12 allows for unambiguous conclusion that the molecular Helmholtz free energy f is linked to the chemical potential as follows:

$$f = \mu - \bar{p}_T V \quad (7)$$

This is the same result obtained previously for the gas adsorption on an open surface (Ustinov and Do 2012a), i.e. the normal pressure is not accounted for despite of the fact that it is comparable to the tangential pressure.

The chemical potential in Eq. (7) can be replaced by $k_B T \varphi$. This is reasonable because the chemical potential undergoes much larger fluctuations than the function φ . Then combining Eqs. (5) and (7) one can obtain the following expression for the molecular Helmholtz free energy:

$$f(a, T) = b + k_B T \int_{a_0}^a a^{-1} \xi da \quad (8)$$

Here the free parameter b can be determined from the dependence $\mu/(k_B T) - \varphi$ shown in Fig. 7 for the disordered branch of the adsorption isotherm. Hence, we can determine the Helmholtz free energy and the internal energy of the adsorbed phase as a function of the chemical potential or amount adsorbed. The former is probably more demonstrable because the chemical potential is constant during ordering transition. The internal energy and the entropy change in the proximity of the 2D phase transition are presented in Fig. 13.

The internal energy plotted in Fig. 13a shows that the interaction potential increases in absolute term with loading in the region of disordered monolayer. The ordering transition appears as a stepwise drop of the internal energy by $\Delta u = -0.241$ kJ/mol. This value seems not significant, but it should be taken into account that the amount adsorbed increases during ordering by $0.60 \mu\text{mol}/\text{m}^2$. Therefore, the change of the total internal energy related to the change of amount adsorbed is -25.07 kJ/mol. This gives the heat of ordering transition of 25.71 kJ/mol, which exceeds the isosteric heat of adsorption just before the transition by 2.15 kJ/mol. Interestingly, after the formation of the ordered monolayer the internal energy decreases with loading, and then increases again with loading. This is because the repulsion is becoming significant due to densification of the hexagonally packed monolayer.

As regard to entropy of the adsorbed phase presented in Fig. 13b, it always decreases with loading reflecting a

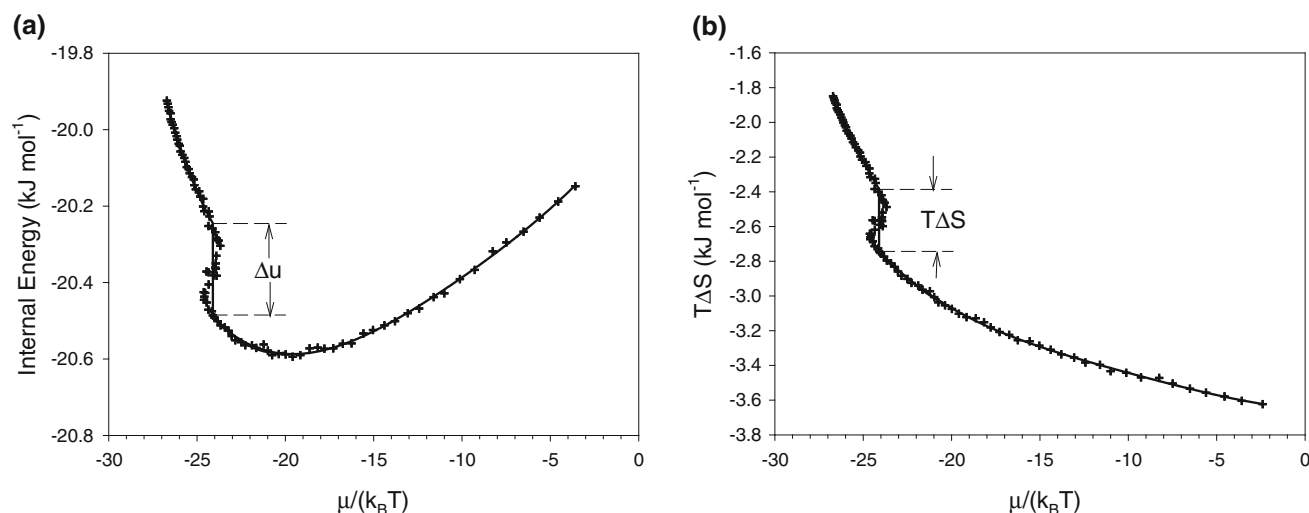


Fig. 13 Internal energy (a) and entropy (b) of argon monolayer adsorbed in a slit pore of 0.679 nm at 77 K in the vicinity of the ordering transition. Vertical steps show the change of thermodynamic function at the ordering transition

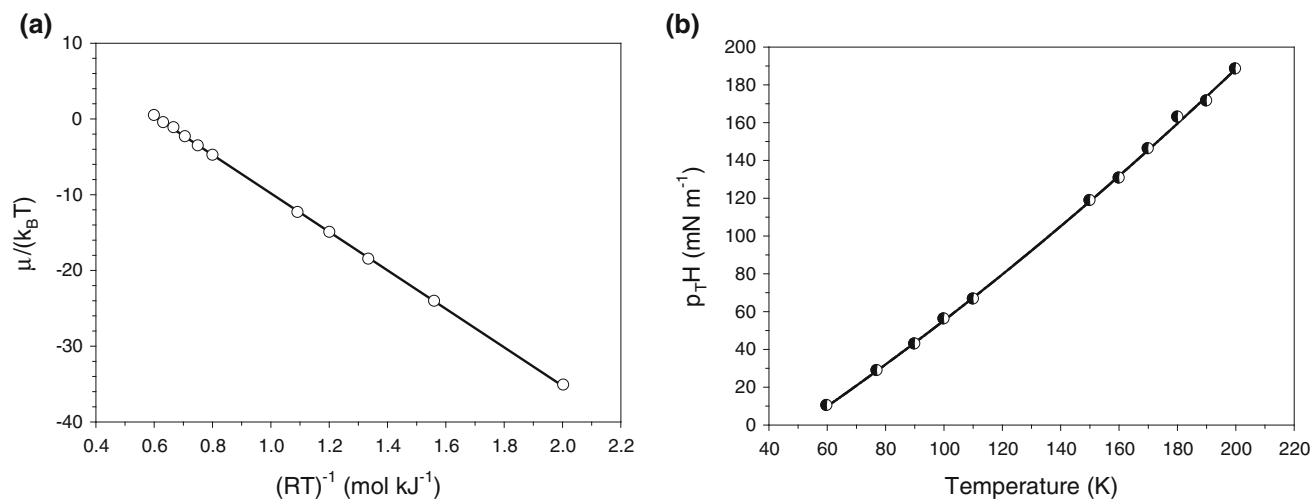


Fig. 14 Effect of temperature on the chemical potential (a) and the tangential pressure (b) of the order–disorder coexistence in the system argon–slit pore of 0.679 nm

gradual loss of freedom for molecules to be in random position within the simulation box volume. As expected, the entropy stepwise drops at the 2D ordering transition.

The effect of temperature on the equilibrium ordering transition is illustrated in Fig. 14 for argon adsorption in slit pore of $2.0\sigma_{ff}$.

The dependence of $\mu/(k_B T)$ on the inverse temperature is nearly straight line over the temperature range from 60 to 200 K (see Fig. 14a) with the slope of -25.4 kJ/mol. Thermodynamically, the slope of this curve in coordinates of Fig. 14a numerically equals to the change in the internal energy during solidification at a given temperature in the system of constant volume related to the change in number of molecules in this system, i.e.

$$\frac{d(\mu/T)}{d(1/T)} = \frac{a_O u_O - a_D u_D}{a_O - a_D} \quad (9)$$

where indexes ‘O’ and ‘D’ denote the coexisting ordered and disordered phases, respectively. The heat of equilibrium melting can be determined with the following equation:

$$\Delta H = \frac{p_T H}{a_D} + u_D - \frac{a_O u_O - a_D u_D}{a_O - a_D} \quad (10)$$

The tangential pressure sharply increases with temperature as seen in Fig. 13b, therefore, in spite of nearly constant value of the right hand side of Eq. (9), the heat of melting significantly changes with temperature.

Thus, the heat of melting is 7.25 kJ/mol at 77 K and 22.0 kJ/mol at 200 K.

The temperature of freezing and melting is usually determined at a specified pressure of the bulk phase (see the paper of Coasne et al. 2009 as an example of a large number of papers on this matter). A more general way, however, is a thermodynamic analysis of the order–disorder coexistence at various temperatures. The equilibrium freezing/melting temperature can be easily determined from a dependence presented in Fig. 14a at any bulk pressure using the following expression for the chemical potential:

$$\mu = k_B T \ln \left(\frac{p \sigma_{ff}^3}{k_B T} \right) \quad (11)$$

Here p is the bulk pressure. The standard chemical potential is omitted for simplicity. It is implied that the bulk phase behaves as the ideal gas, which is correct for the conditions under consideration. Thus, for the bulk pressure of 1 bar the temperature of the hypercritical fluid–solid coexistence in the pore of 0.68 nm is 140.6 K, which coincides with the value obtained by Coasne et al. (2007) for the same system.

The methodology used in this study can be extended to pores of various widths at various temperatures. Thus, we revealed that the 2D hypercritical fluid–solid transition in the pore of width $2\sigma_{ff}$ ($=0.679$ nm) occurs even at 200 K. The effect of pore width on the ordering transition is also important and interesting. Further investigations of adsorption of different gases in slit pores, including the effect of surface defects, on the ordering transition are needed for the refinement fundamental representations of thermodynamic features of the adsorbed phase and also for practical purposes, including the characterization of nanoporous materials.

4 Conclusion

We proposed a new method of modeling gas adsorption on an open homogeneous surface and in graphitic slit pores with the kMC scheme accounting for the ordering transition. The essence of our method in case of the ordered adsorbed phase is a variation of the simulation box size with loading on the basis of Gibbs–Duhem equation. In case of completely ordered adsorbed phase in narrow slit pores the change of the amount adsorbed is achieved only by changing the box volume at a specified number of molecules, with the chemical potential being determined by integration the Gibbs–Duhem equation. This method has allowed for the correct modeling of the adsorption isotherms at a high loading accounting for a significant compressibility of the adsorbed

phase, while the conventional method of simulation in a box of constant volume leads to erroneous appearance of its incompressibility. We thoroughly analyzed thermodynamic properties of the adsorbed phase and derived features of the 2D ordering transition using such thermodynamic functions as the Helmholtz free energy, entropy and internal energy. The results obtained in this study show that some fundamental features associated with adsorption of gases on a homogeneous surface and in slit pores were overlooked and further analysis is needed to deeper understanding the adsorption phenomena.

Acknowledgments This work is supported by Russian Foundation for Basic Research (Project No. 11-03-00129-a). Support from the Australian Research Council is also acknowledged.

References

- Abaza, S., Aranovich, G.L., Donohue, M.D.: Adsorption compression in surface layers. *Mol. Phys.* **110**, 1289–1298 (2012)
- Coasne, B., Jain, S.K., Naamar, L., Gubbins, K.E.: Freezing of argon in ordered and disordered porous carbon. *Phys. Rev. B* **76**, 085416 (2007)
- Coasne, B., Czwartos, J., Sliwinska-Bartkowiak, M., Gubbins, K.E.: Effect of pressure on the freezing of pure fluids and mixtures confined in nanopores. *J. Phys. Chem. B* **113**, 13874–13881 (2009)
- D’Amico, K.L., Bohr, J., Moncton, D.E., Gibbs, D.: Melting and orientational epitaxy in argon and xenon monolayers on graphite. *Phys. Rev. B* **41**, 4368–4376 (1990)
- Demetrio de Souza, J.L.M., Lerner, E.: Melting of argon adsorbed on exfoliated graphite. *J. Low Temp. Phys.* **66**, 367–378 (1987)
- Flenner, E., Etters, R.D.: Behavior of partial monolayers of argon adlayers deposited on graphite. *Phys. Rev. Lett.* **88**, 106101 (2002)
- Flenner, E., Etters, R.D.: Properties of argon adlayers deposited on graphite from Monte Carlo calculations. *Phys. Rev. B* **73**, 125419 (2006)
- Fan, Ch., Razak, M.A., Do, D.D., Nicholson, D.: On the identification of the sharp spike in the heat curve for argon, nitrogen, and methane adsorption on graphite: reconciliation between computer simulations and experiments. *J. Phys. Chem. C* **116**, 953–962 (2012)
- Gardner, L., Kruk, M., Jaroniec, M.: Reference data for argon adsorption on graphitized and nongraphitized carbon blacks. *J. Phys. Chem. B* **105**, 12516–12523 (2001)
- Grillet, Y., Rouquerol, F., Rouquerol, J.: Two-dimensional freezing of nitrogen or argon on differently graphitized carbons. *J. Colloid Interface Sci.* **70**, 239–244 (1979)
- Irving, J.H., Kirkwood, J.G.: The statistical mechanical theory of transport processes. IV. The equations of hydrodynamics. *J. Chem. Phys.* **18**, 817 (1950)
- Kruk, M., Jaroniec, M., Gadkaree, K.P.: Determination of the specific surface area and the pore size of microporous carbons from adsorption potential distributions. *Langmuir* **15**, 1442–1448 (1999)
- Kaneko, T., Mima, T., Yasuoka, K.: Phase diagram of Lennard-Jones fluid confined in slit pores. *Chem. Phys. Lett.* **490**, 165–171 (2010)
- Larese, J.Z., Zhang, O.M., Passel, L., Hastings, J.M.: Layer-by-layer growth of solid argon films on graphite as studied by neutron diffraction. *Phys. Rev. B* **40**, 4271–4275 (1989)

- Long, Y., Palmer, J.C., Coasne, B., Sliwinska-Bartkowiak, M., Gubbins, K.: Pressure enhancement in carbon nanopores: a major confinement effect. *Phys. Chem. Chem. Phys.* **13**, 17163–17170 (2013)
- Migone, A.D., Li, Z.R., Chan, M.H.W.: Melting transition of submonolayer Ar adsorbed on graphite. *Phys. Rev. Lett.* **53**, 810–813 (1984)
- Morrison, J.A.: Calorimetry in the study of physical adsorption. *Pure Appl. Chem.* **59**, 7–14 (1987)
- Rouquerol, J., Partyka, S., Rouquerol, F.: Calorimetric evidence for bidimensional phase change in the monolayer of nitrogen or argon adsorbed on graphite at 77 K. *J. Chem. Soc. Faraday Trans. I*(73), 306–314 (1977)
- Salamacha, L., Patrykiewicz, A., Binder, S., Sokolowski, K.: The structure of fluids confined in crystalline slitlike nanoscopic pores: bilayers. *J. Chem. Phys.* **120**, 1017 (2004)
- Ustinov, E.A., Kukushkina, J.A., Betz, W.R.: Modeling of adsorption of gases on graphite surfaces accounting for the solid–fluid nonadditivity correction. *Langmuir* **27**, 209–214 (2011)
- Ustinov, E.A., Do, D.D.: Thermodynamic analysis of ordered and disordered monolayer of argon adsorbed on graphite. *Langmuir* **28**, 9543–9553 (2012a)
- Ustinov, E.A., Do, D.D.: Application of kinetic Monte Carlo method to equilibrium systems: vapor–liquid equilibria. *J. Colloid Interface Sci.* **366**, 216–223 (2012b)
- Ustinov, E.A., Do, D.D.: Simulation of gas adsorption on a surface and in slit pores with grand canonical and canonical kinetic Monte Carlo methods. *Phys. Chem. Chem. Phys.* **14**, 11112–11118 (2012c)
- Ustinov, E.A., Do, D.D.: Effects of melting and ordering on the isosteric heat and monolayer density of argon adsorption on graphite. *Adsorption* **19**, 291–304 (2013)
- Vishnyakov, A., Neimark, A.V.: Specifics of freezing of Lennard-Jones fluid confined to molecular thin layers. *J. Chem. Phys.* **118**, 7585 (2003)